Jurnal Ilmu Fisika

Wind Gust Parameterization Assessment under Convective and Non-convective Events: A Case Study at the Kertajati International Airport

Muhammad Rafid Zulfikar[1], Muhammad Rais Abdillah[2], Prasanti Widyasih Sarli[3,4]

[1] Undergraduate Program in Meteorology, Faculty of Earth Sciences and Technology. Institut Teknologi Bandung, Bandung, 40132, Indonesia
[2] Atmospheric Sciences Research Group, Faculty of Earth Sciences and Technology, Institut Teknologi Bandung, Bandung, 40132, Indonesia
[3] Structural Engineering Research Group, Faculty of Civil and Environmental Engineering, Institut Teknologi Bandung, Bandung, 40132, Indonesia
[4] Center for Infrastructures and Built Environment, Institut Teknologi Bandung, Bandung, 40132, Indonesia

Article Info	ABSTRACT
  Corresponding Author: Muhammad Rais Abdillah Email: m.rais@itb.ac.id	Wind gusts (gusts) are sudden increases in wind speed that potentially cause severe damage to infrastructure. Gusts occur within several seconds but numerical weather models typically predict future wind with a time step of tens of seconds or minutes. Therefore, a parameterization is needed to estimate gust. Gusts can be produced convectively and non-convectively depending on the presense of thunderstorm. The gust parameterization schemes may perform differently in both cases. In this study, five wind gust parameterization schemes were evaluated at the Kertajati International Airport. Based on simulations of three convective gust and three non-convective gust events using several evaluation metrics, we find that the best scheme for non-convectively driven gusts is the Turbulent Kinetic Energy (TKE) scheme, while the Hybrid scheme performs best for convectively driven gusts. However, the performance of Hybrid scheme during non-convective event is not so far behind TKE scheme. The Hybrid scheme was developed to work on both non-convective and convective events and this capability is evidently shown. The result could be useful to develop mitigation measures for strong wind incident that frequently occurs in Indonesia. *Copyright © 2023 Author(s)*

1. INTRODUCTION

Indonesia grapples with meteorological catastrophes, with extreme weather and powerful wind events frequently leading the list of natural calamities over the past decade, as reported by the National Disaster Management Authority (BNPB, 2022). These wind events inflict substantial harm across communities, vital infrastructure, and crucial sectors, including transportation. Therefore, devising and implementing precise and dependable strong wind forecasts, particularly for gusts, is paramount for risk mitigation (Sarli et al., 2019).

The World Meteorological Organization (WMO) defines gusts as abrupt escalations in wind speed, quantified by the peak three-second average within an observation cycle. Despite their transient nature, gusts can propel light debris, posing risks to people and potential damage to materials and air traffic operations at airports. The turbulent nature of gusts and their effects on structures, such as wind turbines and aircraft, have been examined through computationally demanding Large Eddy Simulations

(LES) with fine resolution (Knigge & Raasch, 2016). An alternative, the mesoscale Weather Research and Forecasting (WRF) model, offers a more resource-efficient approach, albeit at the sacrifice of directly resolving the small-scale turbulent structures that define gusts (Wyngaard, 2004).

Gusts are categorized into non-convective and convective types, each with unique estimation schemes (Sheridan, 2014). Some models, like those proposed by Bechtold & Bidlot (2009), excel in capturing non-convective gusts but may falter in representing those arising from convective systems. Considering the distinct nature of each gust type, it is crucial to develop tailored approaches for both convective and non-convective gusts to enhance forecasting accuracy (Gutiérrez & Fovell, 2018).

Predicting wind events is a complex task, influenced by a plethora of factors such as model initialization, spatial resolution, and the specific parameterization schemes employed (Gutiérrez & Fovell, 2018). Forecasts based on standardized adjustments are not universally applicable, as regional variations can render such models ineffective (Fovell & Cao, 2014). Notably, gust parameterization techniques that have been successfully implemented in regions like Russia, Uruguay, and Europe (Born et al., 2012) might not translate well to the Indonesian context, which is characterized by its distinct climate, weather patterns, and topography.

Indonesia's unique meteorological profile, marked by intense diurnal cycles and prevalent convective activity, suggests that convective gusts may be more common here than in other regions. Furthermore, the archipelago's intricate topography contributes to the unique behavior of gust phenomena within the country. Given these regional specificities, the suitability of existing gust parameterization methods for Indonesia remains unconfirmed, underscoring the need for localized testing to identify the most accurate parameterization for this region.
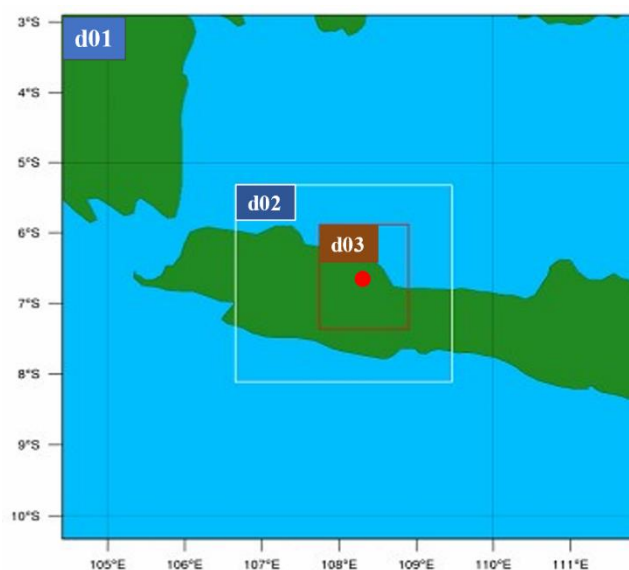
Figure 1 Configuration of 3 nested-domain WRF with spatial resolution of 9, 3, and 1 km, respectively. Domain 1 (d01) is represented by the whole map while domain 2 (d02) is bounded by the white box and domain 3 (d03) is bounded by the red box. The red circle denotes the Kertajati Airport.

Motivated by the distinct meteorological conditions of Indonesia, this research aims to gauge the predictability of wind gusts by scrutinizing a range of parameterization schemes pertinent to both convective and non-convective weather events. Kertajati International Airport serves as the focal point for this evaluation. As a relatively new addition to Indonesia's aviation infrastructure, the microclimate of Kertajati remains largely unexamined, yet the necessity for regular gust predictions is imperative for the safety of flight operations. Recent findings indicate that the Kertajati region experiences higher gust velocities compared to other areas in western Java (Abdillah et al., 2022), suggesting a heightened vulnerability to wind-induced calamities. This study, therefore, seeks to advance our understanding of gust dynamics in this particular region, potentially enhancing the safety and reliability of aviation activities.

2. DATA AND METHOD

2.1 Data

We used weather observation data from an automatic weather station (AWS) close to the Kertajati International Airport. The weather parameters that we obtained are average wind speed, maximum wind speed, and precipitation from 10-min records. The maximum wind speed parameter is used as a proxy for gust data for model evaluation. The observation data availability is April-December 2018 and January-December 2020. The AWS is managed Indonesian Agency for Meteorological, Climatological and Geophysics (Badan Meteorologi, Klimatologi, dan Geofisika or simply BMKG) and the quality control of recorded data was done by Abdillah et al. (2022). The AWS is located on an open area, which is suitable for wind observation (Suomi & Vihma, 2018). The observed wind data is used for events selection and simulated gust evaluation. Three infrared bands of Himawari-8 satellite images (bands 13,14, and 15) are also used to identify gust events associated with convective systems (Bessho et al., 2016). The satellite images have 10-min temporal resolution and 2 km horizontal resolution. National Centers for Environmental Prediction-Final Analysis (NCEP-FNL) (NCEP, 2015) is used as initial and boundary conditions for mesoscale models.

2.2 Selection of convective and non-convective gust cases

Due to limited computation resource, we were only able to simulate several days of gust events instead of conducting a long-term simulation. To select the cases, identification was conducted to determine cases of gust events associated with convective and non-convective. This process consists of looking for cases that had significant gust and clear skies (no precipitation or cloud detected) for non-convective gust cases, and rainy with deep convective cloud for convective gust cases. The condition was chosen based on gust generation process (Rose (NOAA), 2022.; Seman, 2022.; Sheridan, 2014), which convective gust generated by downdraft due to convective systems. To ensure that there is associated convective system, thunderstorm or cumulonimbus cloud detection was conducted using the Himawari-8 satellite images. This was done by utilizing split window method (JMA, 2007), which fulfill the condition as follows:

$$\Delta BT_1 = BT(13) - BT(14) \leq 2 \text{ K} \tag{1}$$

$$\Delta BT_2 = BT(13) - BT(15) \leq 3 \text{ K} \tag{2}$$

$BT(13)$, $BT(14)$, and $BT(15)$ are the brightness temperature from band 13, band 14, and band 15, respectively. Based on the above criteria, three cases of convective gusts and three cases of non-convective gusts were selected (Table 1). Clear skies condition for nonconvective case was chosen to minimalize convective systems effect on gust generation and cumulonimbus detection at potential convective case are conducted on significant gust (gust peaks).

Table 1 List of days selected as convective and non-convective events
and their associated weather condition at Kertajati

Date (in 2018)	Rain event	Cumulonimbus cloud	Avg. *gust* (m/s)	Max. *gust* (m/s)	Case type
21 April	V	V	3.07	15.2	
7 November	V	V	4.10	11.6	Convective
10 December	V	V	3.21	16.4	
1 May	-	-	4.39	7.1	Non-convective
3 June	-	-	2.95	6.8	
14 July	-	-	10.46	14.9	

2.3 WRF Configuration and Simulation

After determining the simulation date, weather simulations using Advanced Research WRF (WRF-ARW) version 4.0 (Skamarock et al. 2019) were carried out using NCEP-FNL data as the model's initial and boundary conditions. The global data contain properties of atmospheric conditions

with a spatial resolution of $0.25° \times 0.25°$ and are available every 6 hours. This simulation utilizes 3 nested-domain downscaling with spatial resolution of 9, 3, and 1 km, respectively (Figure 1). The model output is archived every 10 minutes. Spin-up time that was used in this study was 5 hours that not included in 24-hour simulation of each gust event. Some physical parameterizations that are used in the study are shown in the Table 2. Parameterization schemes from the first two domains refer to the schemes used in the experimental weather forecast system developed by Weather and Climate Prediction Laboratory at Institut Teknologi Bandung (http://weather.meteo.itb.ac.id). As the innermost domain (d03) has a grid resolution of 1 km, which is sufficient for calculating convection explicitly (e.g., Amirudin et al. 2022), the cumulus parameterization at this domain domain was not used.

Table 2 Physical parameterizations configured for the WRF simulation. See WRF Users' Guide from Skamarock et al. (2019) for more details.

Paramaterization schemes	Domain 1	Domain 2	Domain 3
Cumulus	Kain-Fritsch	Kain-Fritsch	-
Microphysics	Lin et al	Lin et al	Lin et al
Planetary Boundary Layer	MYNN	MYNN	MYNN

2.4 Wind Gust Parameterization

As wind gust occurs within the temporal scales that are much shorter than the typical time step of weather simulation (~1 min), we need to perform parameterization of wind gust. Wind gust parameterization in this study is kind of different from the usual physics WRF parameterization such as cumulus, microphysics, or Planetary Boundary Layer (PBL) as shown in Table 2. The parameterization was carried out in a diagnostic and non-interactive way, which mean the quantity was calculated physically but did not give feedback effect to other variable in the model (Goyette et al., 2003). This method was done by estimating the gust dynamically based on WRF output model using five parameterization schemes that were introduced in previous studies. From the five schemes, two schemes were developed for non-convective events (TKE and ECMWF-NC schemes), one scheme was designed for convective events (Brasseur scheme), and two others were built for both convective and non-convective events (Hybrid and ECMWF-NC&C schemes). This study evaluates all the five schemes in both convective and non-convective events to assess and confirm their performances in our study area.

2.4.1 TKE Scheme

This scheme consider TKE (turbulence kinetic energy) in the estimation that represent its wind speed deviation of the average wind speed (Kurbatova et al., 2018). Assuming the wind speed distribution is normal distribution, this estimation was shown in the Equation (3).

$$G = U + 3\sigma \ = U + 3\sqrt{q} \tag{3}$$

where G, U, σ, q are near-surface gust speed, wind speed, standard deviation of wind speed, and TKE, respectively. This method was developed primarily for non-convective gusts.

2.4.2 Brasseur Scheme

The Brasseur Scheme was designed for convective gusts. This scheme assumes that gust is the result of downward air parcel deflection in the boundary layer. This deflection described by the large eddies asufficient enough to transport air parcels to the surface (Brasseur, 2001). The estimation for this scheme is shown in Equation (4):

$$G = \max[U(Z_p)] \tag{4}$$

This equation taking account maximum value of wind speed variation vertically up Z_P to or air parcel height, to explain the air parcel that can reach the surface and carry speed from those levels. The air parcel height was considered if the mean turbulent kinetic energy of large turbulent eddies is greater than the buoyancy energy between the height of the parcel and the surface as follow:

$$\frac{1}{Z_P - Z'} \int_{Z'}^{Z_P} q(z)dz \geq g \int_{Z'}^{Z_P} \frac{\Delta\theta_v}{\emptyset_v}(z)\, dz \quad ; 0 < Z' \leq Z_P \; dan \; Z_P \leq Z_{PBL} \tag{5}$$

Z' is target height (nearest level of anemometer height (10 m) was chosen in this study, Z_P is air parcel height where air parcel moving downward adiabatically to Z', Z_{PBL} is planetary boundary layer height, q is turbulent kinetic energy, g is gravitational acceleration (9.8 m/s^2), $\emptyset_v$ is virtual potential temperature at Z_P level, $\Delta\theta_v$ is virtual potential temperature variation between Z' and Z_P.

2.4.3 Hybrid Scheme

This scheme estimates gust by combining TKE and Brasseur schemes (Kurbatova et al., 2018) and thus it is expected to perform well in both convective and non-convective conditions. It is used by determining atmosphere stability as shown in Equation (6):

$$G = \begin{cases} U + 3\sqrt{q}, \; Ri > 0 \\ \max[U(Z_p)], Ri \leq 0 \end{cases} \tag{6}$$

where R_i is the Richardson number. Negative R_i indicates unstable atmosphere stratification hence Brasseur scheme was used, whereas positive R_i indicates stable atmosphere hence TKE scheme was used. This instability index can be described as the ratio of buoyancy term and flow shear term (Leelőssy et al., 2014; Schnelle, 2003) as shown in the Equation (7):

$$Ri = \frac{\text{Buoyancy Term}}{\text{Flow Shear Term}} = \frac{g}{\rho} \frac{\Delta\rho/_{\Delta Z}}{(\Delta U/_{\Delta Z})^2} \tag{7}$$

g is gravitational acceleration, ρ air density, U is wind speed, and Z is height.

2.4.4 ECWMF-NC Scheme

ECMWF wind gust model have been parameterized as the sum of instantaneous wind speed and a turbulent gustiness that depend of boundary layer static stability until IFS cycle 33r1 (Cy33r1) (Bechtold & Bidlot, 2009). The estimation was designed for non-convective driven gust as shown as follow:

$$G = U + 7.71\, U_* \left[1 + f\left(\frac{z}{L}\right)\right] \tag{8}$$

U is instantaneous wind speed at the target height, U_* is friction velocity, and a function of z or height that affected by turbulence process. The function f is determined by instability index L (Monin-Obukhov length-scale) as shown in the follow equation:

$$f(\tfrac{z}{L}) = \begin{cases} 2.29(1 - \frac{0.5z}{12L})^{1/3}, \; L > 0 \\ 2.29 \qquad\qquad\quad , \; L \leq 0 \end{cases} \tag{9}$$

Monin-Obukhov length-scale is a scale that describe the height where the turbulence was dominantly generated by buoyancy rather than shear. This index estimation is shown as follow:

$$L = -\frac{(-\overline{u'w'})^{\frac{3}{2}}}{k\frac{g}{T}\overline{T'w'}} \tag{10}$$

u', w', T' is zonal wind speed, vertical wind speed, and temperature in the form of turbulence term. T is temperature, g is gravitational acceleration, and k is von karman constant (0.4).

2.4.5 ECMWF-NC&C Scheme

This scheme was an enhanced form ECMWF gust model that considered the effect of deep convective downdraft hence it should be able to predict convectively-driven gust. The convective

component is simply estimated as proportional to the low-level wind shear that added to the Equation (8) as shown in the follow equation:

$$G = U + 7.71\, U_* \left[1 + f\left(\frac{z}{L}\right)\right] + \alpha \max\left(0, U_{850} - U_{950}\right) \tag{11}$$

The value of 0.6 was chosen in this study as α, the tunable 'mixing' parameter. $U_{850} - U_{950}$ is the wind speed difference between the pressure levels of 850 hPa and 950 hPa. If the difference was negative, then zero was chosen as the convective component value or the gust has no contribution from convective processes.

2.5 Model Verification

Verification of simulated gusts was conducted for each case (convective and non-convective) against the observation data and analyzed qualitatively in time series for each day. Quantitative verification was conducted by evaluating through correlation coefficient (r), root mean squared error (RMSE), and mean error (ME) for each case. To minimize the sensitivity of model grids to station location, the model values for evaluation were extracted as a maximum value from 3×3 grids with the center grid are the closest point to observation.

We also evaluate the ability of models in estimating the extreme value of gusts. Extreme gust verification was also carried out since several studies (Gutiérrez & Fovell, 2018; Kurbatova et al., 2018; Nugraha & Trilaksono, 2018) noted that wind gust prediction have underestimate tendency for extreme gust. The extreme gusts were identified by filtering gusts that exceed 95% and 98% percentile. The simulated extreme gusts were then evaluated by looking at the occurrence number and mean magnitude error.
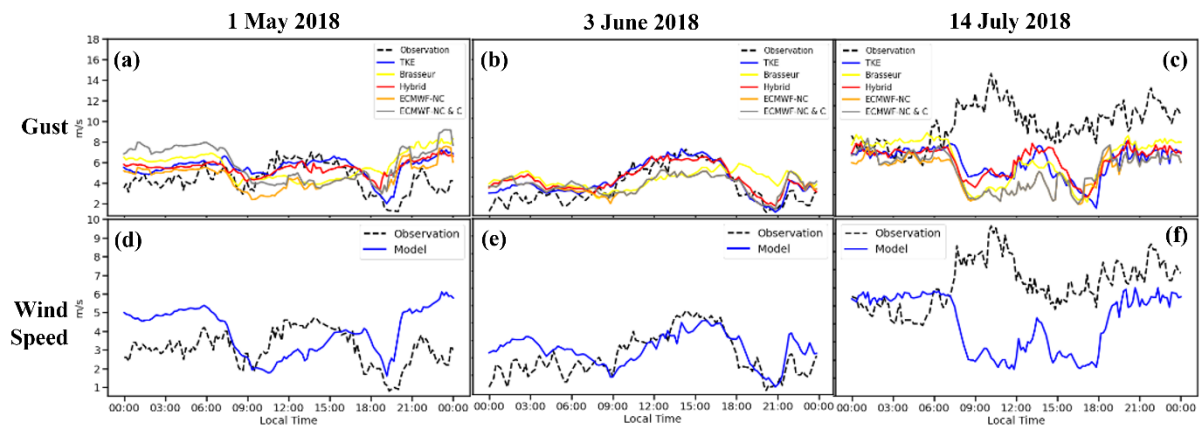
Figure 2 Model and observation (black dashed) of non-convective gust cases time series for: (a), (b), (c) gust and (d), (e), (f) wind speed on: (a), (d) 1 May 2018; (b), (e) 3 June 2018; (c), (f) 14 July 2018.

3. RESULTS AND DISCUSSION

3.1 Evaluation for non-convective gust events

Wind gust estimation for non-convective case show generally good agreement with the observation, especially on the first and second events. On 1 May 2018, ECMWF-NC&C and Brasseur schemes overestimated in the morning and evening, while the other three schemes (TKE, Hybrid, ECMWF-NC) does not differ much with the observations (Figure 2 (a)). In Figure 2 (b) and (e) on the second event, the diurnal pattern of gust and wind is more clear and the overall model performance is better than the first event. Only Brasseur scheme appears to overestimate in the afternoon.

Though the estimated gusts on 14 July 2018 (third event) are very close to the observed gusts in the morning, their relationship began to drop significantly until the midnight, indicating an out-of-phase correlation between the model and the observation (Figure 2 (c)). This is likely due to the inability of the model in predicting the wind speed on that day (Figure 2 (f)) rather than the diagnostic errors

from gust estimation schemes because the gust schemes heavily rely on wind speed values (see Section 2.4). If the diurnal cycle of wind speed is well simulated, then the variation of gust should be good too as demonstrated on the second event (Figure 2 (b) and (e)). This dependency between diurnal wind speed and wind gust performance was also found in previous studies (Kurbatova et al., 2018).
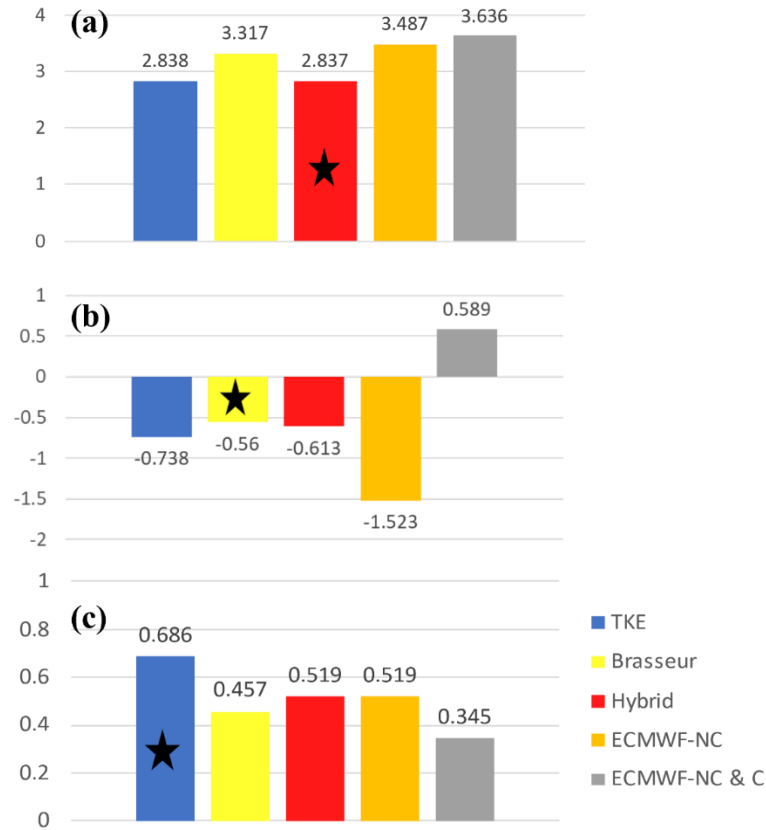
Figure 3 Gust estimation performance comparison for non-convective gust events. Black stars show the best values for (a) RMSE, (b) ME/Bias, (c) correlation coefficients.

Table 3 Extreme gust speed in each percentile (95% and 98%) and its total occurrence count compared to observation percentiles value for non-convective gust case.

Schemes/Observation	95% Percentile		98% Percentile	
	Value (m/s)	Total Occurrence (≥ 12.40 m/s)	Value (m/s)	Total Occurrence (≥ 13.10 m/s)
Observation	12.40	17	13.10	7
TKE	8.10	0	8.30	0
Brasseur	8.90	0	9.12	0
Hybrid	8.13	0	8.37	0
ECMWF-NC	7.47	0	7.78	0
ECMWF-NC&C	8.03	0	8.52	0

Based on quantitative verification, the conclusion seems to be different between RMSE, ME, and correlation for all non-convective events. The smallest RMSE and smallest ME are shown by Hybrid and Brasseur schemes, respectively, while the highest correlation with a considerable margin is achieved by TKE scheme (Figure 3 (a) – (c)). All schemes show mean negative bias except the ECMWF-NC&C that shows mean positive bias (Figure 3 (b)). Interestingly, the ECMWF-NC, which was developed for non-convective gust, shows the worst performance in term of mean bias.
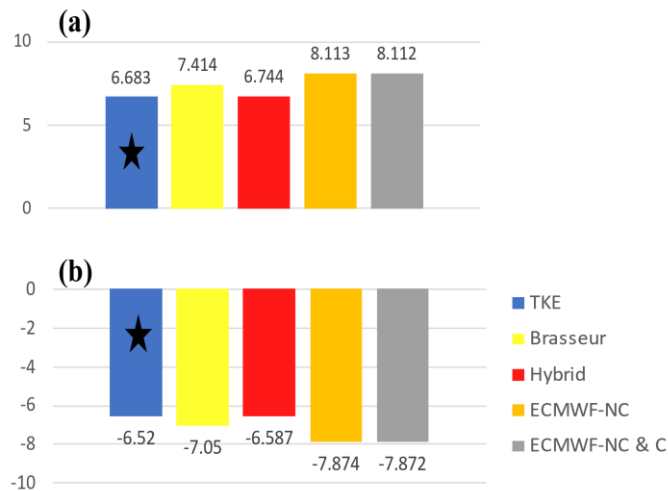
Figure 4 Extreme gust estimation performance comparison for non-convective gust cases. The extreme data was filtered based on the time when the gusts ≥ 12.40 m/s (95% percentile of observation). Black stars show the best prediction for respective verification methods as follows: (a) RMSE and (b) ME/Bias.
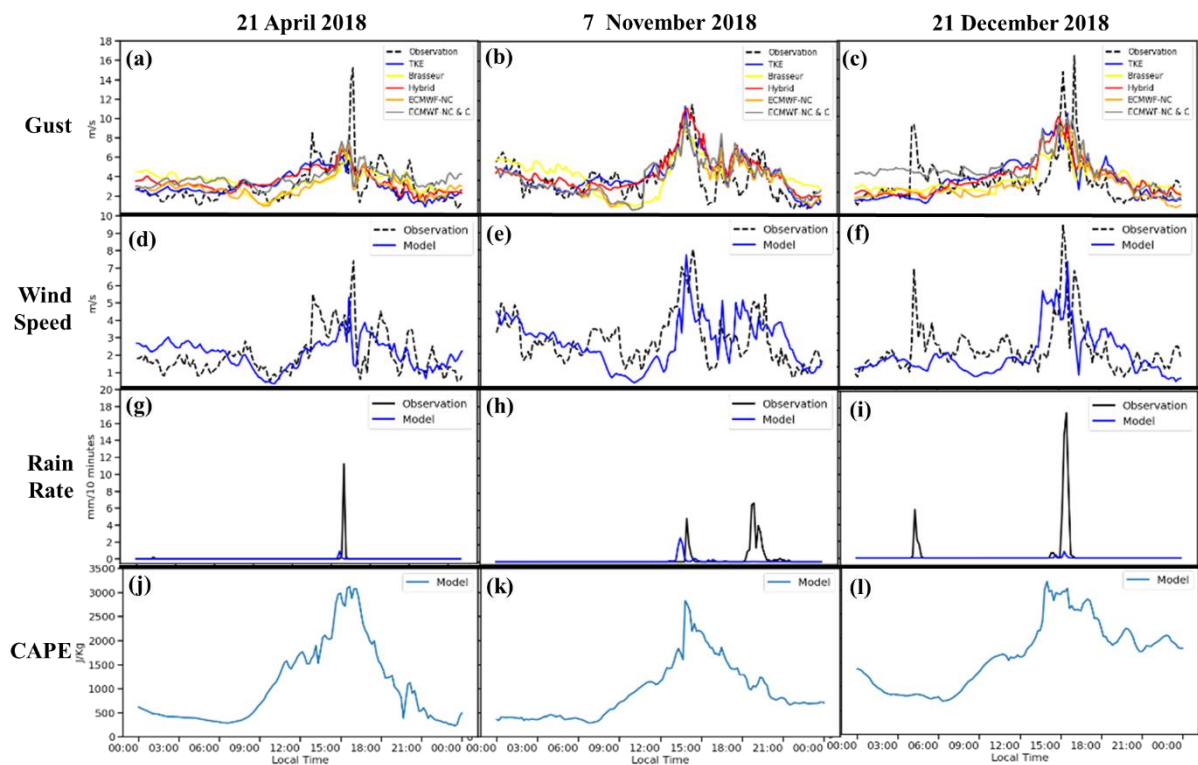
Figure 5 Gust simulation and observation during convective gust events time series for (a) 21 April, (b) 7 November, (c) 10 December 2018. The second row (d-f) and third row (g-i) show simulated and observed wind speed and rain rate, respectively. The fourth row shows CAPE from simulation.

For extreme value comparison during the non-convective events, no schemes estimate extreme gusts as high as the observation and no simulated gusts were detected above the observation extreme thresholds (12.4 and 13.1 m/s) (Table 3). Model thresholds closest to the observation thresholds are depicted by Brasseur schemes (8.9 and 9.12 m/s) but these values are not as different as values in other schemes. Quantitative assessment is done during the observed gusts that exceed 95% percentile (Figure 4). We found that the TKE scheme is superior compared to other schemes in terms of RMSE and ME.

The underestimations are consistent with the previous studies (e.g., Gutiérrez & Fovell, 2018; Kurbatova et al., 2018; Nugraha & Trilaksono, 2018), stressing out the need to carry out further improvement of gust parameterization.

3.2   Evaluation for convective gust events

Convective gust events are associated with deep convective cloud and rain events (see Section 2.2). In general, our gust estimations during these events show good agreement with the observed gusts (Figure 5 (a) – (c)). The model was able to simulate diurnal pattern of gusts, especially on the timing of maximum gusts, which occur in the afternoon. The magnitude of maximum gusts, however, is largely underestimated, except for the second event when the simulated peak was nearly perfect (Figure 5 (b)).
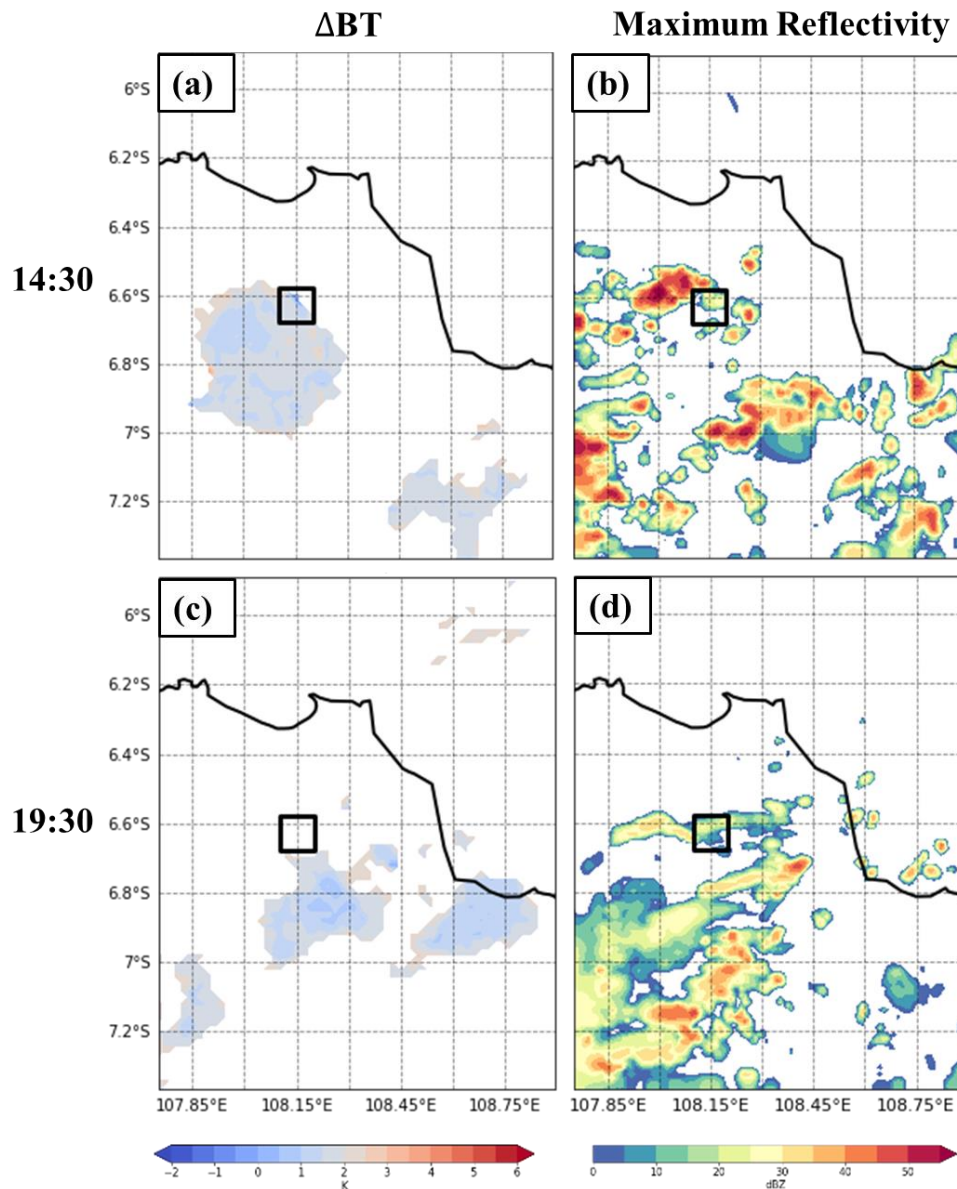
Figure 6 Spatial patterns of (a,c) brightness temperature differences (ΔBT1 masked with ΔBT2 ≤ 3K) from the Himawari-8 and (b,d) simulated maximum reflectivity on 7 November 2018 at (a,b) 14:30 LT and (c,d) 19:30 LT. Black box indicates the station location. Values lower than 2 K in (a,c) indicate cumulonimbus clouds.

The performance of gust simulation seems to be sensitive to the ability of weather model in simulating rainfall event. On the first and third events, the model failed to simulate the rainfall (Figure

5 (g) – (i)), resulting in lower maximum gust and wind speed in the afternoon (Figures 5 (a), (c), (d), (f)). In the second event, however, the afternoon rainfall simulation was much better hence the peak of simulated gust on that day was great at ~15 LT, although the timing of predicted rainfall appeared a bit earlier (Figures. 5b,h).

The timing of daily peak gusts and wind speed that occur in the afternoon was well predicted by the model (Figures 5 (a) – (f)). This is possibly due to the variation of convective available potential energy (CAPE), which is small in the morning and large in the afternoon and early evening (Figures 5 (j) – (l)). Meanwhile the presence of rainfall exerts an impact on modulation of the gust peak, but it gives less impact on the increase in mean wind speed (see the difference on gust and wind speed between model and observation).

It is interesting to note that the second event exhibited two episodes of rainfall (~15 LT and ~20 LT) (Figure 5 (h)). The second rainfall episode was not predicted by the model but the gust comparison during this episode does not differ much (Figure 5 (b)). It is different from that we find on the third event where the missed rainfall event, at early morning, is associated to a large error in gust simulation (Figure 5(c)). We speculate that the presence of small peak of CAPE at 20 LT on the second event (Figure 5(k)), which was absence in the third event at early morning (Figure 5(l)), may maintain the favorable condition for high gust speed in the early evening.
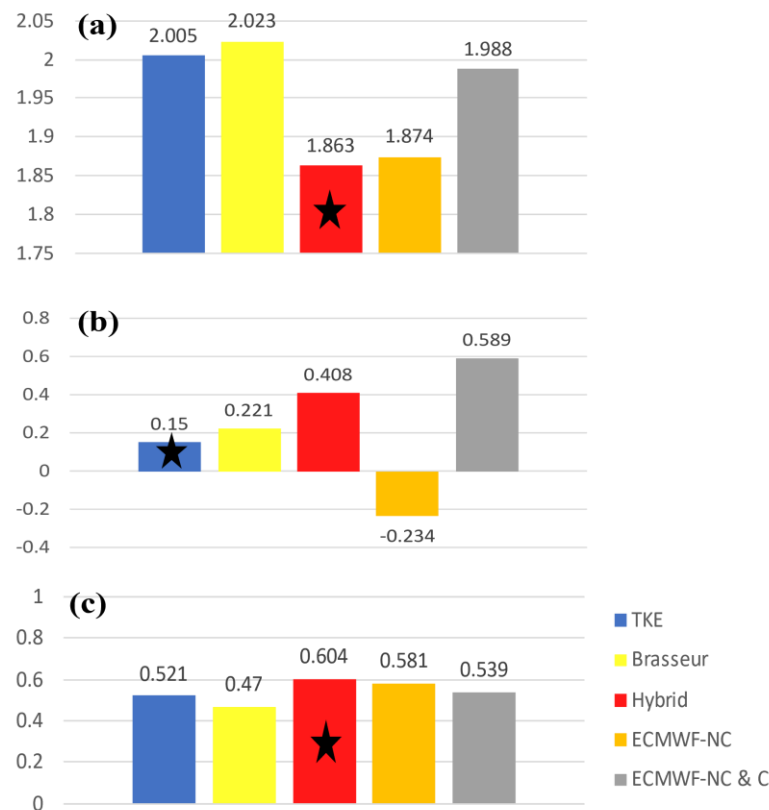
Figure 7 Gust estimation performance comparison for convective gust cases. Black stars show the best prediction for respective verification methods as follow: (a) RMSE, (b) ME/Bias, (c) Correlation.

The role of convective roles is examined further in Figure 6. The figure evidently shows the presence of deep convective activity during the two peaks of gust on the second event. The first peak was driven by a circular convective system in the southwestern side of station location (Figure 6 (a)). The model was able to reproduce the convective system as indicated by very high reflectivity, although the system is a bit smaller and located slightly to the north (Figure 6(b)). On the second peak happened in the early evening, the deep convective cloud was also present close to the station (Figure 6(c)). The

model appeared to also produce high reflectivity during that time but not as high as the reflectivity presented during the afternoon peak (Figure 6(d)). This condition maintained high gust speed in the early evening although the precipitation was not detected.

Figure 7 summarizes quantitative evaluation of simulated gust during convective events from different parameterization schemes. The Hybrid scheme appears to be superior in terms of the highest correlation and the smallest RMSE. The Brasssur scheme that was developed for convective events, unexpectedly, performed worse than others. The ECMWF-NC&C scheme that accommodates the impact of convective events also performed badly. Further analysis is required to investigate the reason.

Table 4 Extreme gust speed in each percentile (95% and 98%) and its total occurrence count compared to observation percentiles value for convective gust case.

Schemes/Observation	95% Percentile		98% Percentile	
	Value (m/s)	Total Occurrence ($\geq$ 7.10 m/s)	Value (m/s)	Total Occurrence ($\geq$ 9.98 m/s)
Observation	7.10	21	9.98	9
TKE	7.04	21	8.26	2
Brasseur	6.26	13	7.54	0
Hybrid	7.45	29	9.32	5
ECMWF-NC	6.78	16	8.28	1
ECMWF-NC&C	7.19	23	8.65	1

Interestingly, the evaluation of extreme gust values during convective events are much better than the those during non-convective events (Tables 3 and 4). It is surprising since numerical models usually suffer in simulating deep convective events in the tropics (e.g., Yulihastin et al., 2021). The TKE scheme shows a better performance of the extremes greater than 95% percentile. However, in a higher percentile threshold, the Hybrid scheme is very close to the observation while all the other schemes largely underestimated (Table 4). The Hybrid scheme shows an extreme limit of 9.32 m/s (98% percentile), close to the observed value of 9.98 m/s. And 5 out of 9 extreme occurrences were detected by the Hybrid scheme while the others only predicted 0, 1 or 2 occurrences. The superiority of the Hybrid scheme is more evident in Figure 8, which shows the smallest errors of Hybrid scheme compared to the others.
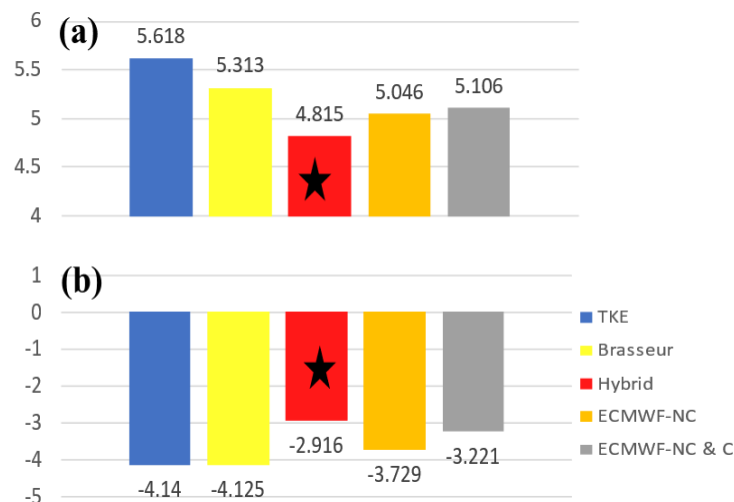
Figure 8 Extreme gust estimation performance comparison for convective gust cases. The extreme data was fitered based on the time when the gusts $\geq$ 7.10 m/s (95% percentile of observation). Black stars show the best prediction for respective verification methods as follows: (a) RMSE and (b) ME/Bias.

4. CONCLUSION

The present investigation contributes to the development of mitigation strategies for the prevalent strong wind incidents in Indonesia by rigorously evaluating various gust parameterization methods. Our analysis at Kertajati Airport has established the Hybrid scheme as a promising approach for predicting gust events across both convective and non-convective conditions. While the TKE scheme exhibited a slight edge during non-convective events, the Hybrid scheme's versatility makes it the recommended choice for operational forecasting, given its design to address both convective and non-convective situations effectively.

Our findings also underscore that gust predictions are influenced by multiple factors beyond the choice of parameterization scheme. Notably, accurate reproduction of mean wind speed variations is crucial during non-convective events, while convective energy and precipitation are pivotal in convective scenarios. This research highlights additional aspects that require enhancement in modeling to achieve improved gust simulations.

Future explorations are necessary to reinforce these findings, as our simulation encompassed only a few days within a confined region. A broader and more extended study would bolster confidence in determining the optimal parameterization method for gust forecasting in Indonesia and might uncover further areas for research advancement.

ACKNOWLEDGEMENT

REFERENCE

Abdillah, M. R., Sarli, P. W., Firmansyah, H. R., Sakti, A. D., Fajary, F. R., Muharsyah, R., & Sudarman, G. G. (2022). Extreme Wind Variability and Wind Map Development in Western Java, Indonesia. *International Journal of Disaster Risk Science*, *13*(3), 465–480. https://doi.org/10.1007/s13753-022-00420-7

Amirudin, A. A., E. Salimun, M. Zuhairi, F. Tangang, L. Juneng, M. S. F. Mohd, and J. X. Chung, 2022: The Importance of Cumulus Parameterization and Resolution in Simulating Rainfall over Peninsular Malaysia. Atmosphere, 13, 1557, https://doi.org/10.3390/atmos13101557.

Bechtold, P., & Bidlot, J.-R. (2009). *Parametrization of convective gusts*. https://doi.org/10.21957/KFR42KFP8C

Bessho, K., Date, K., Hayashi, M., Ikeda, A., Imai, T., Inoue, H., Kumagai, Y., Miyakawa, T., Murata, H., Ohno, T., Okuyama, A., Oyama, R., Sasaki, Y., Shimazu, Y., Shimoji, K., Sumida, Y., Suzuki, M., Taniguchi, H., Tsuchiyama, H., … Yoshida, R. (2016). An Introduction to Himawari-8/9—Japan's New-Generation Geostationary Meteorological Satellites. *Journal of the Meteorological Society of Japan. Ser. II*, *94*(2), 151–183. https://doi.org/10.2151/jmsj.2016-009

BNPB (Badan Nasional Penanggulangan Bencana). 2022. Data and Information of Disasters in Indonesia (Data Informasi Bencana Indonesia-DIBI). Jakarta Timur, Indonesia: Badan Nasional Penanggulangan Bencana.

Born, K., Ludwig, P., & Pinto, J. G. (2012). Wind gust estimation for Mid-European winter storms: Towards a probabilistic view. *Tellus A: Dynamic Meteorology and Oceanography*, *64*(1), 17471. https://doi.org/10.3402/tellusa.v64i0.17471

Brasseur, O. (2001). Development and Application of a Physical Approach to Estimating Wind Gusts. *Monthly Weather Review*, *129*(1), 5–25. https://doi.org/10.1175/1520-0493(2001)129<0005:DAAOAP>2.0.CO;2

Fovell, R. G., & Cao, Y. (n.d.). *5A.2 Wind and Gust Forecasting in Complex Terrain*. 10.

Goyette, S., Brasseur, O., & Beniston, M. (2003). Application of a new wind gust parameterization: Multiscale case studies performed with the Canadian regional climate model: APPLICATION OF A WIND GUST PARAMETERIZATION. *Journal of Geophysical Research: Atmospheres*, *108*(D13), n/a-n/a. https://doi.org/10.1029/2002JD002646

Gutiérrez, A., & Fovell, R. G. (2018). A new gust parameterization for weather prediction models. *Journal of Wind Engineering and Industrial Aerodynamics*, *177*, 45–59. https://doi.org/10.1016/j.jweia.2018.04.005

Knigge, C., & Raasch, S. (2016). Improvement and development of one- and two-dimensional discrete gust models using a large-eddy simulation model. *Journal of Wind Engineering and Industrial Aerodynamics*, *153*, 46–59. https://doi.org/10.1016/j.jweia.2016.03.004

Kurbatova, M., Rubinstein, K., Gubenko, I., & Kurbatov, G. (2018). Comparison of seven wind gust parameterizations over the European part of Russia. *Advances in Science and Research*, *15*, 251–255. https://doi.org/10.5194/asr-15-251-2018

Leelőssy, Á., Molnár, F., Izsák, F., Havasi, Á., Lagzi, I., & Mészáros, R. (2014). Dispersion modeling of air pollutants in the atmosphere: A review. *Open Geosciences*, *6*(3). https://doi.org/10.2478/s13533-012-0188-6

NCEP-National Centers for Environmental Prediction/National Weather Service/NOAA/U.S. Department of Commerce. 2015, updated daily. NCEP GDAS/FNL 0.25 Degree Global Tropospheric Analyses and Forecast Grids. Research Data Archive at the National Center for Atmospheric Research, Computational and Information Systems Laboratory. https://doi.org/10.5065/D65Q4T4Z. Accessed 1 January 2022

Nugraha, A. A. A., & Trilaksono, N. J. (2018). *Simulation of wind gust – Producing thunderstorm outflow over Mahakam block using WRF*. 020051. https://doi.org/10.1063/1.5047336

Rose (NOAA), M. A. (n.d.). *Downbursts*. NOAA's National Weather Service. Retrieved 15 July 2022, from https://www.weather.gov/ohx/downbursts

Sarli, P. W., M. R. Abdillah, and A. D. Sakti (2020): *Relationship between wind incidents and wind-induced damage to construction in West Java, Indonesia*. IOP Conf. Ser.: Earth Environ. Sci., 592, 012001, https://doi.org/10.1088/1755-1315/592/1/012001.

Schnelle, K. B. (2003). Atmospheric Diffusion Modeling. In R. A. Meyers (Ed.), *Encyclopedia of Physical Science and Technology (Third Edition)* (pp. 679–705). Academic Press. https://doi.org/10.1016/B0-12-227410-5/00036-3

Seman, S. (n.d.). *Single-Cell Thunderstorms | METEO 3: Introductory Meteorology*. Retrieved 15 July 2022, from https://www.e-education.psu.edu/meteo3/l8_p5.html

Sheridan, P. (2014). *Forecasting Research Technical Report 570*. 22.

Skamarock, William C, Joseph B Klemp, Jimy Dudhia, David O Gill, Dale M Barker, Michael G Duda, Xiang-Yu Huang, Wei Wang, and Jordan G Powers (2019). *A Description of the Advanced Research WRF Version 3*. Colorado: NCAR.

Wyngaard, J. C. (2004). Toward Numerical Modeling in the "Terra Incognita". *Journal of the Atmospheric Sciences*, *61*(14), 1816–1826. https://doi.org/10.1175/1520-0469(2004)061<1816:TNMITT>2.0.CO;2

Yulihastin, E., D. E. Nuryanto, Trismidianto, and R. Muharsyah, 2021: Improvement of Heavy Rainfall Simulated with SST Adjustment Associated with Mesoscale Convective Complexes Related to Severe Flash Flood in Luwu, Sulawesi, Indonesia. *Atmosphere*, 12, 1445, https://doi.org/10.3390/atmos12111445.